SCIENTIFIC REPORTS

Mechanosensitive physiology of *chlamydomonas reinhardtii* under direct membrane distortion

Seul Ki Min[1], Gwang Heum Yoon[1], Jung Hyun Joo[1], Sang Jun Sim[2] & Hwa Sung Shin[1]

[1]Department of Biological Engineering, Inha University, Incheon, 402-751, Korea, [2]Department of Chemical and Biological Engineering, Korea University, Seoul, 136-713, Korea.

Cellular membrane distortion invokes variations in cellular physiology. However, lack of an appropriate system to control the stress and facilitate molecular analyses has hampered progress of relevant studies. In this study, a microfluidic system that finely manipulates membrane distortion of *Chlamydomonas reinhardtii* (*C. reinhardtii*) was developed. The device facilitated a first-time demonstration that directs membrane distortion invokes variations in deflagellation, cell cycle, and lipid metabolism. *C. reinhardtii* showed a prolonged G_1 phase with an extended total cell cycle time, and upregulated Mat3 regulated a cell size and cell cycle. Additionally, increased TAG compensated for the loss of cell mass. Overall, this study suggest that cell biology that requires direct membrane distortion can be realized using this system, and the implication of cell cycle with Mat3 expression of *C. reinhardtii* was first demonstrated. Finally, membrane distortion can be an attractive inducer for biodiesel production since it is reliable and robust.

Biochemical stimuli such as osmolality, pH, and temperature induce cytoskeleton remodeling, growth, and changes in cell cycle[1,2]. The resulting physiological variations are often reflected by variations in the mechanical properties of cellular membranes. For example, yeast alters their cytoplasm to glass transition and loses protein motility in response to osmotic pressure[3]. Similarly, tobacco pollen tubes shrank or swelled in response to osmotic stress (hypo- or hyper-) and developed abnormal specific phospholipid signals[4]. In recent years, mechanical stresses exerted on the cell membrane have been recognized to highly affect cellular physiology[5,6]. Indeed, stretching- or compression-driven membrane distortion has been reported to be associated with cellular mechanotransduction, which transduces extrinsic mechanical stress to intracellular signaling networks[6,7]. Despite recent extensive efforts, mechanotransduction via signal transduction of membrane distortion to intracellular biological variations is still not well understood. Thus, it is necessary to develop novel methodologies such as an adequate cell model and apparatus to control membrane distortion to elucidate the effects of membrane distortion on intracellular cytoskeleton remodeling, growth, cell cycle, and self-defense behaviors.

Growth and cell cycle are pivotal to analysis of cellular physiology, and cyclin-dependent kinases (CDKs) are central among a conserved set of proteins that regulate cell cycle phase transitions[8]. Retinoblastoma protein (RB) plays a key role as a cell cycle regulator that inhibits the transcription of genes required for the cell cycle while linking regulatory genes for S-M phase transition and CDKs[9]. The RB-related pathway is conserved in plants, animals, and green algae, but not in yeast and fungi. The unicellular green microalgae, *C. reinhardtii*, possess cell cycle proteins including the Mat, a Rb homologue, pathway, which are highly similar to plants and vertebrates; however, its division shows multiple fission via a noncanonical mechanism[10]. Moreover, unlike in higher plants and animals in which they undergo extensive duplication, the cell cycle genes of *C. reinhardtii* have been reported to exist as a single copy[11]. For these reasons, *C. reinhardtii* has long been recognized as a system for investigation of the cell cycle of higher eukaryotes, as well as for biodiesel production[12]. A few trials have been conducted to investigate the physiological variations of *C. reinhardtii* under membrane distortion. Mechanosensitive ion channels (MSCs) or their homologues exist in *C. reinhardtii* to sense mechanical stimuli. Previous studies reported that MSCs activated by membrane distortion caused variations of molecular phenomena and morphology via mechanotransduction[13]. For example, Yoshimura suggested that patch clamp-assisted negative pressure applied to the membrane of *C. reinhardtii* induced an increase in single ion-current via excessive inflow of calcium[14]. Additionally, MSC1 in the cytoplasm and chloroplast of *C. reinhardtii* is related to organization of chloroplast, and the presence or absence of the N-terminal signal sequence of MSC1 may vary depending on cell membrane stretching[15]. Similarly, many phenomenological and morphological studies have reported changes in

the cell organelle by MSC activation induced by membrane distortion of *C. reinhardtii*[14]. However, no studies have investigated physiological aspects of the cell cycle related to mechanotransduction. To investigate the effects of direct membrane distortion on the cell cycle and growth, intracellular signaling proteins and transcripts should be investigated; therefore, it is necessary to develop a device capable of controlling membrane distortion to a specific amount of cells at one time and location for microscopic assessment of morphological changes and intracellular protein remodeling, as well as to facilitate statistical analyses of biochemical events of cells at the proteomic and transcript level.

Using currently available mechanical stress inflicting systems based on agarose gel[16] or shear stress[17], it is difficult to generate direct membrane distortion of cells and to impart the same mechanical stress on all cells. Systems using patch clamps are able to lead and control direct membrane distortion; however, it is difficult to apply the same stress to many cells at one time and to conduct proteomic and transcript-level studies using such systems[14]. A report describing cell cycle analysis of *C. reinhardtii* using a microfluidic culture system was recently published, but this study was not related to the effects of mechanical stresses[18]. To date, there have been no studies conducted to investigate effects of direct membrane distortion on cells in a transcript level. Therefore, in this study, we developed a microfluidic device capable of applying the same compressive stress to many cells at one time in one space. We then discussed the membrane distortion effects on the cell cycle that occurred through mechanotransduction and the subsequent changes that occurred in lipid metabolism.

Results

Design of a microfluidic device generating direct membrane distortion in *C. reinhardtii*. A microfluidic device that applies compressive stress on a specific amount of *C. reinhardtii* cells was fabricated as shown in Fig. 1a. Height is a critical parameter in effective application of stress to cells. To determine the adequate height for compression of cells, cellular volume was measured and

calculated. Confocal images of three-dimensional cells were captured as they were fully grown and immediately after they divided into daughters (Fig. 1b). The smallest daughter cells were found to have an average volume of 60.46 μm^3. Theoretically, if the smallest daughter cell had a ball shape, the diameter would be 4.87 μm. Therefore, the channel of the device must have height < 4.87 μm. For a typical demonstration experiment, the device used in this study consisted of 133 channels that were 100 μm in width, 2–2.5 μm in height, and 20 mm in length, with a pillar 50 μm wide and 20 mm long between channels, and two reservoirs on both sides of the device (Fig. 1). To judge from the result that the red dye in one side reservoir diffused across channels to the other reservoir within 1 day, cells in the channels were not affected from limitation of nutrient (Supplementary Fig. 2). As shown in Fig. 1c, the daughter cell was completely compressed and successfully underwent its own cell cycle. The degree of the membrane distortion was expressed by cellular strain that was calculated by equation 1[22]. As a result, the compressed cell showed 35% of strain compared with uncompressed one (Supplementary Fig. 3).

$$\varepsilon_p = \frac{l_e - l_0}{l_0} = \frac{d_e - d_0}{d_0} \qquad (1)$$

Compressive stress causes deflagellation via a calcium influx mediated pathway. The first typical phenotypic change in response to compression in the device is deflagellation of the *C. reinhardtii*. As shown in Fig. 2a, *C. reinhardtii* were deflagellated immediately after compression (yellow triangles), but reflagellation occurred with the lapse of time during 2 h (red triangles). Deflagellation of *C. reinhardtii* has been shown to be related to calcium influx through the cellular membrane and remodeling of the actin filament[19,20]. Figure 2b and 2c shows the microscopic image and spectroscopic intensity of Ca^{2+} in cells. As expected, the intracellular fluorescent intensity of Fura-2 was much higher in the compressed cells 2 h after compression. The compressed cells also
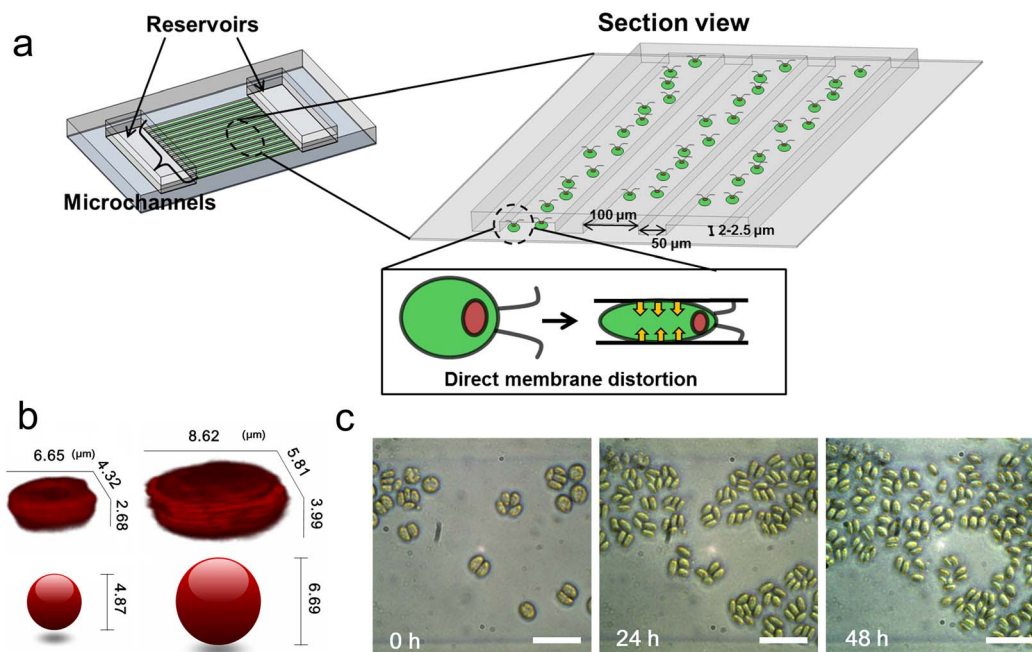

Figure 1 | Design of a microfluidic device generating direct membrane distortion on *C. reinhardtii*. (a) Schematic design of a microfluidic device exerting compressive stress and strain on *C. reinhardtii* and cross-sectional image of the channels (Actual dimensions were noted but the figure were not shown as actual ratio). (b) Confocal images of *C. reinhardtii* were captured as a daughter was immediately hatched out from a mother cell (left) and fully grown (right). Below are balls that have the same volume as the above corresponding cell. (c) Successful cell growth and division in the microfluidic device. Scale bars, 30 μm.
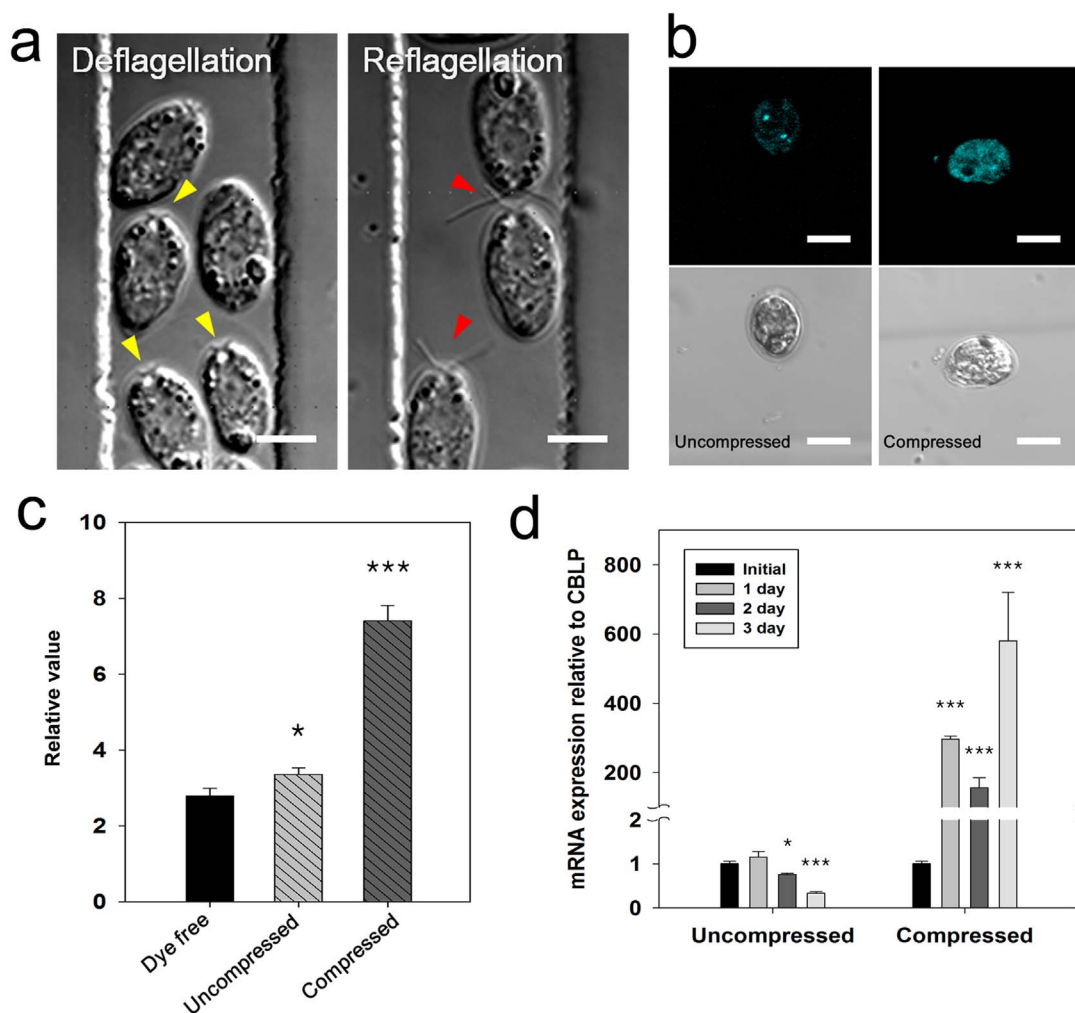
Figure 2 | Deflagellation caused by direct membrane distortion via a Ca²⁺ influx-mediated pathway. (a) *C. reinhardtii* were deflagellated immediately after compression (yellow triangles), but reflagellation occurred with the lapse of time (red triangles). Scale bars, 10 μm. (b) Fluorescent microscopic detection of Fura-2 inside cells that indicates influx of Ca²⁺ ion. Scale bars, 5 μm. (c) Fluorescent spectroscopic measurement of Fura-2. A dye free sample was measured as a background control. (d) Actin mRNA was quantified by RT-qPCR and normalized with CBLP, a housekeeping gene. (* $P < 5.0 \times 10^{-2}$, ** $P < 1.0 \times 10^{-2}$, *** $P < 1.0 \times 10^{-3}$).

synthesized higher levels of actin mRNA transcript than uncompressed cells (Fig. 2d). Taken together, these findings imply that membrane distortion induced a large influx of Ca²⁺ and upregulation of actin mRNA of the compressed cells, resulting in deflagellation.

Cell growth and cell cycle of uncompressed or compressed *C. reinhardtii.* Cell growth and cell cycle were assessed by microscope and flow cytometer. During every light-dark cycle, the number of compressed cells increased stepwise (Fig. 3a). The variation in cell number inferred that cell divisions of the compressed cells occurred strictly during the dark period. The cell images and FACS data in Fig. 3b, c and Supplementary Fig. 4 were taken over 24 h. Cell division occurred within 12 h in the both cases (uncompressed and compressed), but the FACS data was different each other at 12 h. For uncompressed cell, the fraction of cell cycle was divided into two main peaks. The distribution of cell number was gradually crowded in G_1 phase at 24 h and 48 h compared with the initial time because *C. reinhardtii* in normal state had 16 h for total cell cycle time as known by Vitova M. et al[21] (Fig. 3c and Supplementary Fig. 4). However, among the compressed cells, a large number of cells were still in the S/M phase, but a small fraction was in the G_1 phase at 12 h, even though daughter cells were detected within 12 h (Fig. 3b, d), and the growth pattern was stepwise every 24 h

(Fig. 3a). These mean that total cell cycle time was extended up to around 24 h longer than uncompressed cells. Additionally, most daughter cells hatched out within 12 h under compression were in S/M phase at 24 h, but many uncompressed daughter cells were already in G_1 phase. This indicates that G_1 phase of compressed *C. reinhardtii* has been prolonged.

Cell size control of direct membrane distortion and its implications with upregulated Mat3 expression. The physiological activities of daughter cells under compressive stress and strain need to be investigated during the cell cycle. Therefore, the cell size, daughter cell number and Mat3 mRNA, and E2F1 mRNA expression were evaluated. Compressed and uncompressed daughter cells that hatched out between 12 and 24 h were measured at 36 h, when the cells were fully grown and just before division. The compressed cells showed a much smaller size than the uncompressed ones, but were smaller than the early phase of the uncompressed daughter cells at 12 and 24 h (Fig. 4a). The number of daughter cells was also compared immediately after they were just hatched out at around 40 h (Fig. 4b). The compressed cells had higher fission number than uncompressed cells (P < 0.001). As shown in Fig. 4c, compressed cells had greatly upregulated mRNA of Mat3, while E2F1 expression level was not different from that of uncompressed cells at 24 h.
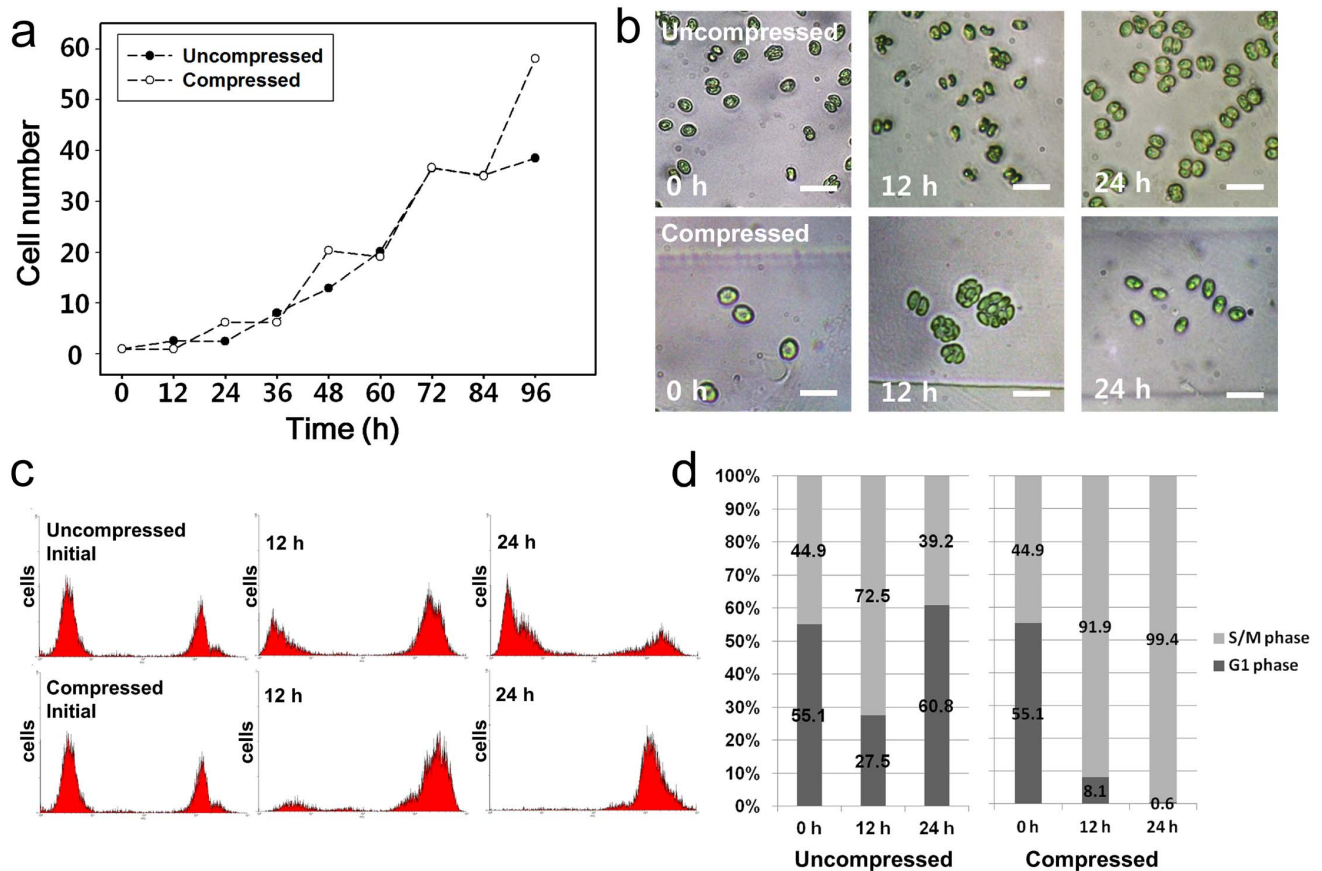
Figure 3 | Growth and cell cycle of *C. reinhardtii* under direct membrane distortion. (a) Cell growth patterns during every light-dark cycle. (Light : 0–12 h, 24–36 h, 48–60 h, 72–84 h, Dark : 12–24 h, 36–48 h, 60–72 h, 84–96 h) (b) Cell division that was observed every 12 h. (c) FACS-assisted cell cycle that was identified every 12 h. (d) The distribution of cell cycle phases that was expressed as percentages of cell number.

Overcoming environmental limitations of *C. reinhardtii* cultured in the microfluidic device. The compressed cells were stained with 1 µM Sytox Green and their microscopic images were taken using a fluorescence confocal microscope. *C. reinhardtii* cultured under compressive stress for 1, 2, 3 d showed viability of 93.6%, 93.7% and 96.9%, respectively. Considering cells under pillar had been taken necrosis, these results mean apoptotic cells were rarely detected (Fig. 5a). Cells were tested under more strict conditions of a width of 20 µm. The cells successfully underwent their cell cycle and divided into daughter cells, and finally occupied the entire area of the channel (Fig. 5b). These imply that cells in the narrow and wide microchannels were healthy and thus underwent proper cell division and metabolic activities without apoptosis.
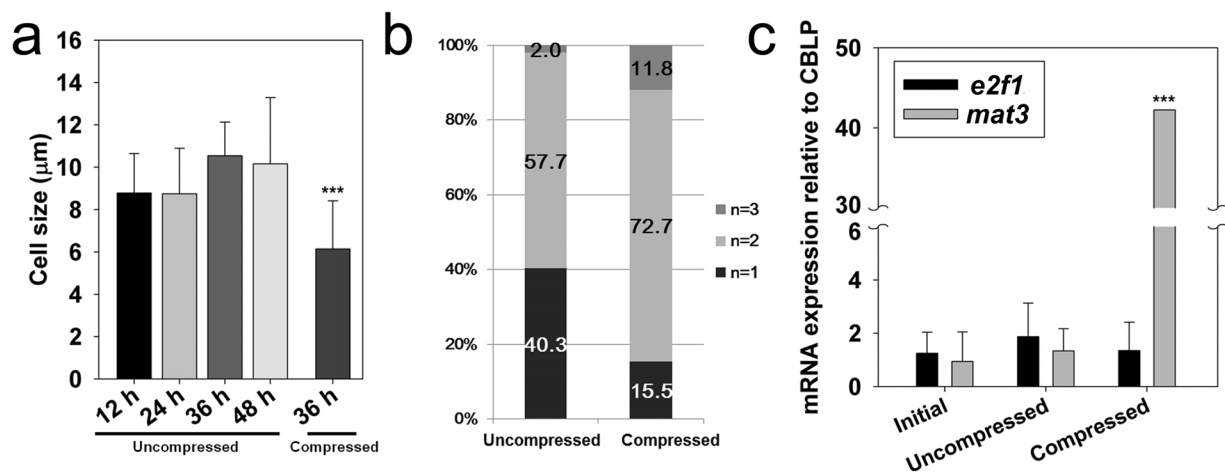

Figure 4 | Cell size control of direct membrane distortion and its implications with expressions of Mat3 and E2F1. (a) Cell size of the compressed *C. reinhardtii* that were fully grown and just before cell division (at 36 h). (b) Comparison of multiple fission of *C. reinhardtii* between uncompressed and compressed conditions (at 40 h) (n; fission number). (c) Mat3 and E2F1 mRNA was quantified by RT-qPCR and normalized with CBLP, a housekeeping gene. (* $P < 5.0 \times 10^{-2}$, ** $P < 1.0 \times 10^{-2}$, *** $P < 1.0 \times 10^{-3}$).
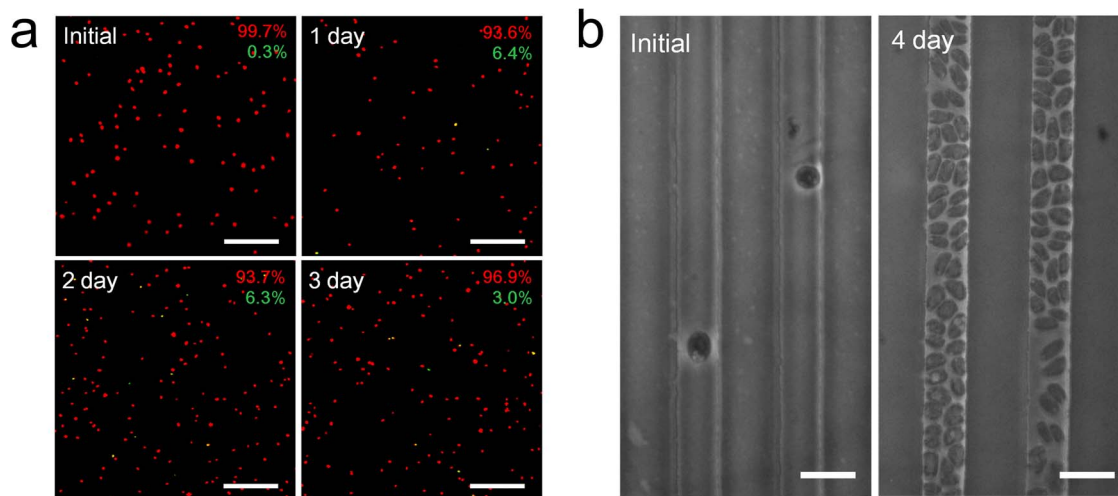
Figure 5 | Apoptosis analyses of *C. reinhardtii* cultured in the microfluidic device. (a) Apoptosis analysis of *C. reinhardtii* by Sytox green staining. The percentages of viable and apoptotic cells were indicated on the upper right (Red; auto-fluorescence of viable cells, Green; dead cells). Scale bars, 100 μm. (b) Cell growth of *C. reinhardtii* that were grown in the narrow width channel. Scale bars, 20 μm.

A novel inducer, direct membrane distortion, upregulating lipid accumulation. Environmental stresses increase TAG accumulation inside microalgae. To investigate the effects of direct membrane distortion on the TAG synthesis pathway, Nile red-stained TAG was monitored by fluorescence microscope every 4 h and quantified by image analysis of its intensity. As shown in Fig. 6a, the size or number of lipid bodies increased significantly when compared with uncompressed cells. To confirm whether the lipid bodies were induced only by the compression, microscopic image of the compressed cells intact in microchannels (2–2.5 μm height) without collection was compared with ones intact in non-compressing microchannels (50 μm height) (Supplementary Fig. 5). Lipid bodies were detected in the compressed cells intact but were negligible in the uncompressed ones, similar to those of the collected samples as seen in Fig. 6a. The time required for lipid metabolism to respond to the mechanical signal via membrane distortion was progressed within 4 h as seen in Supplementary Fig. 6. After 3 days of cultivation, lipid bodies were maintained inside the cells without degradation or release (Fig. 6a). Additionally, mRNA of DGAT, LPAAT and ACCase was measured, which were known to be related to free fatty acids, PtdOH, and TAG syntheses (Supplementary Fig. 7). The three genes relevant to lipid synthesis were found to be upregulated under compressive stress during day 1 (Fig. 6c).

Discussion

A microfluidic device that facilitates biochemical analyses of membrane-distorted *C. reinhardtii* physiology must meet several requirements. First, a reliable control parameter is necessary so that the level of membrane distortion can be finely manipulated. Additionally, the culture volume should be sufficient to harvest cells for biochemical analyses and to permit nutrients and gases to flow smoothly. Finally, it should be made of visible materials to allow real-time monitoring of cell morphology. The system shown in Fig. 1a satisfies all of these requirements. Membrane distortion can be controlled by adjusting the height of PR patterning of the wafer for the microfluidic device. The wide width (100 μm) of the device enables cells to proliferate and operate their metabolism normally without any problem in media exchanging. Polydimethylsiloxane (PDMS) is commonly used as a transparent and gas-permeable material and thus real-time monitoring and gas-exchange must be guaranteed. Even though the simple design does not appear to have any novel characteristics, the simplicity of the culture system and ability to control parameters ensures equal and simultaneous distortion level in membranes of all cultured cells, resulting in increased reliability of the experimental results. Membrane deformation could be ascertained upon observation of cells grown under this system (Fig. 1c) as a result of direct contact of the cell membrane and the device. Moreover, the wide channel width allows cells to undergo 3 cell cycles inside the device. Some trials of microfluidic compression of mammalian cells[22] and yeast[23] have been conducted; however, there have been no reports of transcript-level data describing cellular physiology. To the best of our knowledge, this device and application provide the first transcript-level data describing cellular behavior under direct membrane distortion. By the way, to confirm from procedures for preparing the device, there are no typical differences of mechanical and nutrient stresses between cells in flask and uncompressed cells in channels with height greater than cell size. So, uncompressed cells cultured in flask was used as a control to compare with compressed cells. This result provides not only comparing cell physiology directly under direct membrane distortion with pre-existing results that have been performed in flask culture, but also it highlights the efficacy of membrane distortion as a novel inducer for lipid synthesis. The typical microscopic events that occur in *C. reinhardtii* under stresses such as low pH, osmotic pressure, and shear stress are deflagellation and flagellar excision, which have been widely reported to be associated with Ca^{2+} influx via extracellular and intracellular pathways[24]. Several studies have reported signaling pathways of deflagellation after Ca^{2+} influx, which include katenin, Nima family kinase, and inositol phospholipid metabolism-mediated signaling[25]. Ca^{2+} influx invokes flagellum beating that is known to occur via flagella dynein[26]. Since actin is one of the components of inner arm dynein, mutated genes encoding actin invoked a defect in assembly of inner arm dynein[27]. Therefore, Ca^{2+} influx is expected to influence the expression of actin mRNA. However, deflagellation of *C. reinhardtii* under direct membrane distortion has rarely been investigated, even though patch clamp-assisted negative pressure applied to *C. reinhardtii* uncovered rapid Ca^{2+} influx through the mechanosensitive channel (MSC)[14]. In the present study, application of direct compressive stress to *C. reinhardtii* was found to induce Ca^{2+} influx. Actin mRNA was analyzed to demonstrate the efficacy of the device for transcript-level investigation of cells. Actin mRNA was successfully found to be upregulated as the cellular membrane was exposed to direct compressive stress, which has been impossible in systems that employ patch clamps and indirect mechanical stress. However, increased actin mRNA is also observed in *C. reinhardtii* subjected to
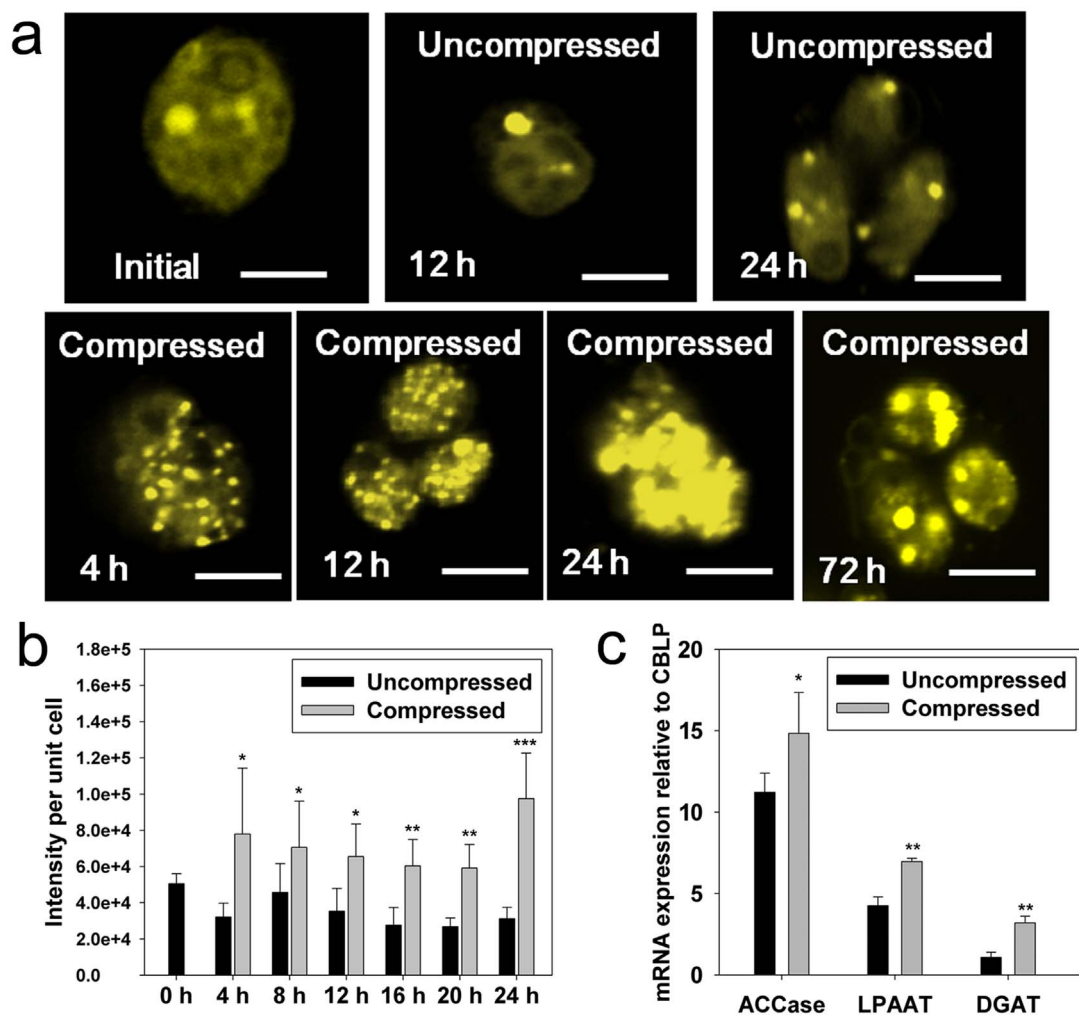
Figure 6 | Upregulation of lipid synthesis of *C. reinhardtii* under direct membrane distortion. (a) Temporal changes in the formation of lipid bodies in the uncompressed and compressed cells based on Nile red staining. Scale bars, 5 μm. (b) Quantification of intensities of lipid bodies based on an average of 40 cells. (c) DGAT, LPAAT, and ACCase mRNA were quantified by RT-qPCR and normalized with CBLP, a housekeeping gene. (* $P < 5.0 \times 10^{-2}$, ** $P < 1.0 \times 10^{-2}$, *** $P < 1.0 \times 10^{-3}$).

low pH[19,28]. Therefore, deflagellation-related phenomena under direct membrane distortion to *C. reinhardtii* could be very similar to that under indirect membrane distortion caused by low pH, osmotic pressure, and N deprivation.

Calcium influx, actin reorganization, and deflagellation are known to be coupled with cell cycle[29,30]. Therefore, knowledge of the cell cycle of *C. reinhardtii* should enable a broad understanding of the cell's physiology under mechanical stress. The cell cycle mechanism of *C. reinhardtii* has been investigated while focusing on the Mat signaling pathway[10,11,31,32], and the results revealed that the Mat pathway regulates cell cycle and size control signals and is incorporated with E2F1, DP1, and smt[10]. Following Umen's work[9], in *mat3*-deleted *C. reinhardtii*, G_1 phase was prolonged and total cell cycle time was preserved, but cell division occurs in a smaller state and produces many more daughter cells with a smaller size. Interestingly, these results are similar to the cell cycle pattern of *C. reinhardtii* under direct membrane distortion except the extended total cell cycle time in this work: cells divided in a much smaller state and more daughter cells with smaller size were produced compared to uncompressed cells. In addition, the number of daughter cells from compressed cells was between the number of daughter cells of uncompressed cells and *mat3*-deleted cells. Based on the *mat3*-deleted mutants, the prolonged G_1 phase facilitates a longer replication cycle, resulting in many more daughter cells that are smaller in

size. This explains our finding that smaller cells divided into many more daughter cells that were also smaller in size because G_1 phase were prolonged also in this work. However, upregulated Mat3 was also different from that of the *mat3* deleted mutant. Mat3, E2F1, DP1, and smt are known cell size regulators in *C. reinhardtii*[10]. Despite the possible effects of DP1 and smt on the cell cycle of *C. reinhardtii* independently of E2F1, previous studies have shown that their activities in the cell cycle are incorporated with E2F1[10]. Based on the fact that no significant differences exist in the E2F1 mRNA level between compressed and uncompressed cells, but that Mat3 is upregulated in compressed cells, Mat3 could be believed to operate as a cell size regulator under compressive stress rather than E2F1, DP1, and smt do. Additionally, even though no studies were performed in this work, Mat3 might also work for cell cycle regulator under direct membrane distortion, because G_1 phase were prolonged in this work and Rb has been known to regulate cell cycle in mammalian cells[33]. Nevertheless, the unique phenomenon of Mat3 upregulation of the compressed cells needs to be further analyzed in view of cell cycle including apoptosis. Many researchers have reported that Rb plays an anti-apoptotic role in an upregulated state[34]. If Mat3 plays the same role in *C. reinhardtii*, Mat3 may express a similar upregulated response to apoptosis. However, as shown in Fig. 5, an active cell cycle was detected, even in the narrow-width microchannel, which can lead to more compressive stress. Several previous studies have

reported that upregulated E2F1 is related to apoptosis[35]. However, no significant variations in E2F1 mRNA were observed between compressed and uncompressed cells. Therefore, all these findings signified that Mat3 upregulation is not thought to be related with apoptosis and the compressed cells adapted their physiology to the compressive stress and altered their metabolism to survive. On the other hand, Tang reported that HEK 293 cells upregulated Rb expression when membrane tension increased in response to hypoosmotic stress[36]. Osmotic stress invoked membrane distortion and induced phenomena similar to direct membrane distortion such as Ca^{2+} influx. Accordingly, the upregulation of Mat3 mRNA in this study is intuited to be consistent with the results of previous studies and is asserted to be an adequate response to assure cell size and cell cycle under the direct membrane distortion. Nevertheless, the signaling studies should be further conducted using *mat3*-knock out model to identify the implications of upregulation of Mat3 with cell size and cycle. Judging from the smaller mature cells but prolonged total cell cycle time under direct membrane distortion, the metabolic activity for cell growth of the compressed cells was down-regulated when compared with uncompressed cells. This raises the question of where the remaining metabolic flux went. That is, the overall physiological phenomena of compressed cells indicate that a significant flux must have been transferred in a direction other than toward accumulation of cell mass through active growth and cell cycling so that the loss of cell mass could be compensated for. This energy may have been transferred to TAG, which is believed to be dependent on increased free fatty acids in chloroplasts or increased transformation toward PtdOH and DAG and finally TAG. Lv et al. investigated transcriptome analysis in the course of lipid accumulation and suggested LPAAT and DAGAT are significantly upregulated by up to 1.76 and 1.44 times, respectively[37]. Oelkers et al. reported that DGAT is an important regulator of lipid synthesis by facilitating combination of the third acyl-CoA to the diacylglycerol molecule[38]. Moreover, CO_2 uptake and synthesis of free fatty acids in chloroplast precede the synthesis pathway of TAG in *C. reinhardtii*, where Acetyl-CoA carboxylase (ACCase) is a key enzyme catalyzing reactions in the chloroplast[39]. Importantly, ACCase, LPAAT, and DAGAT were all upregulated under compressive stress, resulting in upregulated syntheses of free fatty acids, PtdOH, DAG, and TAG. Therefore, the increased TAG was due to increased free fatty acids in the chloroplast and increased transformation toward TAG in cytosol. High light intensity, pH, nitrogen deprivation, and osmotic stress are known inducers that facilitate lipid metabolism at the expense of cell mass[40]. These factors can be assumed to exert similar effects on the physiology of *C. reinhardtii*. Investigations of nitrogen stress have revealed that it results in lipids being highly synthesized, but growth of chlorella vulgaris being decreased[41]. Taken together, these findings indicate that cells transfer their potential for growth to lipid synthesis so that they can resist stressful environments. TAG of microalgae is drawing attention as an upcoming next-generation biofuel due to its easy conversion to biodiesel. To date, the methods used to induce high synthesis of TAG have been nitrogen deprivation, temperature, pH, and osmotic pressure. However, these might cause uncontrollability and non-robustness during mass production owing to their complexity and mass transfer limitations. In contrast, compression is a simple mechanical method that has greater controllability and robustness, even in large-scale processes.

Mechanotransduction provokes unique phenomena in morphology via cytoskeleton remodeling and in the cell cycle through signaling pathways such as ERK, CDK, Rb, and cellular metabolism in response to mechanical stress. In this study, we first demonstrated the effects of direct membrane distortion on cellular morphology, cell cycle, and lipid metabolism using *C. reinhardtii*. Direct membrane distortion provoked deflagellation via Ca^{2+} influx and upregulation of actin, as well as disturbance in the cell cycle leading to prolonged cell cycle time and G_1 phase and many daughter cells of

smaller size. Additionally, the compressed cells operated their metabolic pathways very actively without apoptosis and expressed high amounts of lipids at the expense of cell mass.

Methods

Fabrication of a microfluidic device. As shown in Fig. 1a, a microfluidic device was fabricated by soft lithography. Briefly, SU-8 2 (MicroChem), a negative photoresist (PR), was coated onto 4 inches of silicon wafer for 30 sec at 1350 rpm to give a final height of 3 μm according to the manufacturer's guide. After pre-baking at 60°C for 1 min and then at 95°C for 3 min, the device was subjected to UV light for 10 sec to induce cross-linking. The device was then subjected to post-baking on post plate at 60°C for 3 min and 95°C for 3 min, after which the film was put on a PR-coated silicon wafer. The wafer was subsequently washed with propylene glycol monomethyl ether acetate (PGMEA) (Sigma-Aldrich) to develop the pattern and isopropyl alcohol (IPA). The fabricated structure on si wafer master was observed by a white-light interferometer (NewView™, ZYGO) (Supplementary Fig. 1). PDMS (Sylgard 184, Dow corning) solution with curing agent at a ratio of 10 : 1 was subsequently poured onto the device, which was then placed in an oven at 60°C for 4 h. PDMS was able to be tiered from the si wafer master and then reservoirs were formed by using a PDMS punch.

Culture of Chlamydomonas reinhardtii. Wild-type *C. reinhardtii* strain cc-124 was cultured in a shaking incubator (120 rpm) at 23°C under a 12 h light and 12 h dark cycle for synchronization. TAP media (Gibco) was used as a basal media for the cell culture. Cell mass was estimated by the optical density at 680 nm using a spectrophotometer (Tecan). 2 ml of *C. reinhardtii* (O.D. 1.8 at 680 nm) was subcultured into 18 ml fresh TAP media one day before all the assays. All procedures for culturing and harvesting cells in the microchannel used a softly-softly approaches to avoid mechanical agitation as belows. After oxygen plasma treatment on the surface of the glass and microfluidic device, the culture fluid of *C. reinhardtii* (O.D. 1.8 at 680 nm) was slowly dropped onto the glass. Then, the dry parts of glass were automatically attached to the device due to the treatment of oxygen plasma, and cells in wet part were compressed by the roofs of microchannels. To prevent the cells from limitation of nutrients, the *C. reinhardtii* was fed with fresh media from reservoirs on both sides of the microchannel, which were replaced every day. For control experiments, the same microalgae (cc-124) were cultured in a flask (Uncompressed) at the same time. To harvest cells from the device, the device channel was softly cut with a blade. Most of the cells were not attached and easily harvested, but the cells that weakly attached on the glass were gently scraped off.

Cell proliferation. To determine cell growth, the cell number was determined by direct counting from cell images obtained from the same spot by microscope (Micros). Cells were seeded immediately after the dark phase started, and the first cell number was determined after twelve hours. The specific cell number was then calculated by as follows: cell number (at each time)/cell number (at initial). For enumeration of cells cultured in flasks, samples were fixed with gram iodine (10 : 1 v/v) and then counted using a hemocytometer.

Viability and apoptosis of C. reinhardtii. The cultured cells were harvested and stained with 1 mM Sytox Green (Molecular Probes) in TAP media for 10 min at room temperature. A confocal laser microscope (LSM 510 META) was used at 488 nm (Ar-laser)/505–530 nm (excitation/emission) for live cells and at 543 nm (HeNe-laser)/560 nm (excitation/emission) for dead cells. Dual fluorescence images were merged through ZEN 2009 Light Edition software (Carl Zeiss). At least 500 cells in random field at ×100 magnification were calculated for viability and apoptosis at each day.

Cell size distribution. The *C. reinhardtii* cc-124 was seeded in the microfluidic device at the beginning of the dark phase and then harvested after 36 h. Next, the collected cells were centrifuged at 13,500 g for 20 sec, after which they were fixed with 0.25% glutaraldehyde (Sigma-Aldrich) in PBS. Finally, the cell size was measured with a Cellometer Auto T4 Cell Counter (Nexcelom Bioscience) (n > 50).

Cell cycle analysis by FACS. The *C. reinhardtii* cc-124 in the microfluidic device was sampled at 12 h intervals and fixed in 500 μl PBS containing 0.25% glutaraldehyde. Prior to FACS analysis, cellular DNA was stained with 5 μM Sytox Green for 10 min in the dark. A DB FACS Caliburflow cytometer (BD Biosciences) was used for the analysis of the relative DNA fluorescence content. The emission of fluorescence was measured in FL3 channels upon excitation. For all samples, 1×10^5 cells were measured per sample at a pressure of 1 psi. The distribution of cell cycle phases was expressed as percentages of the total number of cells using the WinMDI software (Joseph Trotter, The Scripps Research Institute).

Identification of cytosolic free Ca^{2+} influx. Fura-2 (Sigma-Aldrich) was used to detect the intracellular Ca^{2+} concentration[42]. Briefly, the culture fluid of *C. reinhardtii* (O.D. 1.8 at 680 nm) was centrifuged at 13,500 g for 20 sec and then suspended in NMG^+/K^+ buffer (5 mM HEPES, 10 mM HCl, 1 mM KCl, 200 μM K^+ BAPTA, adjusted with N-methyl-D-glucamine (NMG) to pH 5.6 containing 1 mM sulfinpyrazone) containing 1 mM sulfinpyrazone (Sigma-Aldrich) and 3 μM Fura-2 dissolved in DMSO (Sigma-Aldrich). The suspended cells were seeded in the microfluidic device with the same method as above. After incubation for 2 h at 36°C,

buffer in the reservoirs of the device was discarded and TAP media was added and discarded after 5 min. After repeating this procedure three times, the dye-free NMG^+/K^+ buffer (pH 6.8) was added and incubated for 10 min at $4°C$ in the dark, and then the samples were again centrifuged and loaded into the 96 well plate. Finally, the quantitative fluorescence was measured using a spectrofluorometer (Varioscan) at 340 nm and 380 nm for excitation and 510 nm for emission. The relative intensity of Ca^{2+} was calculated by the ratio of the fluorescence value at 340 nm over 380 nm (Fluorescence 340 nm/Fluorescence 380 nm). For the relative intensity of Ca^{2+} per cell mass, the relative value of Ca^{2+} intensity was divided by the optical density value of cells that was measured by a spectrophotometer at 680 nm. The image of Fura-2-Ca^{2+} in the compressed cell was captured by confocal microscope after repeating that discarding and injecting NMG^+/K^+ buffer (pH 6.8) three times and incubation for 10 min at $4°C$ in the dark without harvesting.

Measurement of lipid in *C. reinhardtii* by Nile red staining. Nile Red (Sigma-Aldrich) staining was performed to observe the changes in lipid production in response to mechanical stress. Briefly, *C. reinhardtii* were seeded in a fabricated microfluidic chip and then sampled every 4 h for 1 day, after which they were fixed with 2.5% glutaraldehyde. The samples were then collected, mixed with Nile Red dye (2 μg/ml) at a 3 : 1 ratio and incubated for 10 min at $40°C$ in the dark. Finally, images of lipid bodies were obtained by a confocal microscopy at an excitation wavelength of 543 nm and an emission wavelength of 630 nm, and the quantitative intensities were measured using the Image J software (US National Institutes of Health).

cDNA Synthesis and Real-Time qPCR. Real time qPCR was conducted to determine the expression level of mRNA. The specific primer sequences and conditions used in this experiment are listed in Table S1. Total RNA was collected using an RNeasy Plant Mini Kit (Qiagen) according to the manufacturer's instructions, with DNease I (Qiagen) being added at the washing step. After verifying no degradation of the RNA by electrophoresis in 1% agarose gels containing Safe Shine Green (Biosesang), the sample was used for synthesis of cDNA. The mixing ratio of reagents was prepared according to the manufacturer's description. Nuclease free water filled into the mixture consisted of 2X SYBR in QuantiFast SYBR Green PCR Kit (Qiagen) and 1 mM each primer up to 20 μl. The data expressed in the form of delta-delta Ct ($2^{-\Delta\Delta 2_T}$) was quantified using the Rotor-Gene Q Series Software (Qiagen). Finally, the delta-delta Ct ($2^{-\Delta\Delta 2_T}$) value was normalized with respect to the expression level of CBLP, a housekeeping gene.

Statistical analysis. All experiments were conducted in triplicate and differences between groups were identified by a student's t-test, with p values (* $P < 5.0 \times 10^{-2}$, ** $P < 1.0 \times 10^{-2}$, *** $P < 1.0 \times 10^{-3}$) taken to indicate significance.

1. Tzur, A., Kafri, R., LeBleu, V. S., Lahav, G. & Kirschner, M. W. Cell growth and size homeostasis in proliferating animal cells. *Science* **325**, 167–171 (2009).
2. Mitchison, J. Growth during the cell cycle. *Int Rev Cytol* **226**, 165–258 (2003).
3. Miermont, A. *et al.* Severe osmotic compression triggers a slowdown of intracellular signaling, which can be explained by molecular crowding. *P Natl A Sci* **110**, 5725–5730 (2013).
4. Zonia, L. & Munnik, T. Osmotically induced cell swelling versus cell shrinking elicits specific changes in phospholipid signals in tobacco pollen tubes. *Plant Physiol* **134**, 813–823 (2004).
5. Patwari, P. & Lee, R. T. Mechanical control of tissue morphogenesis. *Circ Res* **103**, 234–243 (2008).
6. Orr, A. W., Helmke, B. P., Blackman, B. R. & Schwartz, M. A. Mechanisms of mechanotransduction. *Dev Cell* **10**, 11–20 (2006).
7. Zhou, J., Wang, B., Zhu, L., Li, Y. & Wang, Y. A system for studying the effect of mechanical stress on the elongation behavior of immobilized plant cells. *Colloids Surfaces B* **49**, 165–174 (2006).
8. Bisova, K., Krylov, D. M. & Umen, J. G. Genome-wide annotation and expression profiling of cell cycle regulatory genes in Chlamydomonas reinhardtii. *Plant Physiol* **137**, 475–491 (2005).
9. Umen, J. G. & Goodenough, U. W. Control of cell division by a retinoblastoma protein homolog in Chlamydomonas. *Gene Dev* **15**, 1652–1661 (2001).
10. Fang, S.-C. & Umen, J. G. A suppressor screen in chlamydomonas identifies novel components of the retinoblastoma tumor suppressor pathway. *Genetics* **178**, 1295–1310 (2008).
11. Fang, S.-C., de los Reyes, C. & Umen, J. G. Cell size checkpoint control by the retinoblastoma tumor suppressor pathway. *Plos Genet* **2**, e167 (2006).
12. Merchant, S. S., Kropat, J., Liu, B., Shaw, J. & Warakanont, J. TAG, You're it! Chlamydomonas as a reference organism for understanding algal triacylglycerol accumulation. *Curr Opin Biotech* **23**, 352–363 (2012).
13. Morris, C. E. Mechanosensitive ion channels. *J Membr Biol* **113**, 93–107 (1990).
14. Yoshimura, K. Mechanosensitive channels in the cell body of Chlamydomonas. *J Membr Biol* **166**, 149–155 (1998).
15. Nakayama, Y., Fujiu, K., Sokabe, M. & Yoshimura, K. Molecular and electrophysiological characterization of a mechanosensitive channel expressed in the chloroplasts of Chlamydomonas. *P Natl Acad Sci USA* **104**, 5883–5888 (2007).
16. Bouten, C. C., Knight, M., Lee, D. & Bader, D. Compressive Deformation and Damage of Muscle Cell Subpopulations in a Model System. *Ann Biomde Eng* **29**, 153–163 (2001).
17. Moore, J., Jr. *et al.* A device for subjecting vascular endothelial cells to both fluid shear stress and circumferential cyclic stretch. *Ann Biomed Eng* **22**, 416–422 (1994).
18. Matsumura, K., Yagi, T., Hattori, A., Soloviev, M. & Yasuda, K. Using single cell cultivation system for on-chip monitoring of the interdivision timer in Chlamydomonas reinhardtii cell cycle. *JN* **8**, 23 (2010).
19. Hirono, M., Uryu, S., Ohara, A., Kato-Minoura, T. & Kamiya, R. Expression of conventional and unconventional actins in Chlamydomonas reinhardtii upon deflagellation and sexual adhesion. *Eukaryot cell* **2**, 486–493 (2003).
20. Lefebvre, P. A., Silflow, C. D., Wieben, E. D. & Rosenbaum, J. L. Increased levels of mRNAs for tubulin and other flagellar proteins after amputation or shortening of Chlamydomonas Flagella. *Cell* **20**, 469–477 (1980).
21. Vítová, M. *et al.* Chlamydomonas reinhardtii: duration of its cell cycle and phases at growth rates affected by temperature. *Planta* **234**, 599–608 (2011).
22. Kim, Y. C., Park, S.-J. & Park, J.-K. Biomechanical analysis of cancerous and normal cells based on bulge generation in a microfluidic device. *Analyst* **133**, 1432–1439 (2008).
23. Oh, S. *et al. Unraveling mechano-stress responsive signaling networks in budding yeast via microfluidic devices.* Date of access: 29/12/2012 (2012).
24. Quarmby, L. M. & Hartzell, H. C. Two distinct, calcium-mediated, signal transduction pathways can trigger deflagellation in Chlamydomonas reinhardtii. *J Cell Biol* **124**, 807–815 (1994).
25. Chamberlain, K. L. *Gene Expression Profiling of Flagellar Length Control in Chlamydomonas reinhardtii. Diss. Dept. Of Biological Sciences-Florida State University* Date of access: 11/04/2007 (2007).
26. Ken-ichi, W. *et al.* Calcium-dependent flagellar motility activation in Chlamydomonas reinhardtii in response to mechanical agitation. *Cell Motil Cytoskel* **66**, 736–742 (2009).
27. Silflow, C. D. & Lefebvre, P. A. Assembly and motility of eukaryotic cilia and flagella. Lessons from Chlamydomonas reinhardtii. *Plant Physiol* **127**, 1500–1507 (2001).
28. Quarmby, L. *et al.* Inositol phospholipid metabolism may trigger flagellar excision in Chlamydomonas reinhardtii. *J Cell Biol* **116**, 737–744 (1992).
29. Parker, J. D. K. *Co-ordinate regulation of cilia and the cell cycle in Chlamydomonas reinhardtii. Diss. Dept. Of Biological Sciences-Simon Fraser University* Date of access: 14/10/2008. (2008).
30. Mahjoub, M. R. *et al.* The FA2 gene of Chlamydomonas encodes a NIMA family kinase with roles in cell cycle progression and microtubule severing during deflagellation. *J Cell Sci* **115**, 1759–1768 (2002).
31. Cross, F. R. & Roberts, J. M. Retinoblastoma protein: Combating algal bloom. *Curr Biol* **11**, R824-R827 (2001).
32. Olson, B. J. *et al.* Regulation of the Chlamydomonas cell cycle by a stable, chromatin-associated retinoblastoma tumor suppressor complex. *Plant Cell* **22**, 3331–3347 (2010).
33. Cooper, S. & Shayman, J. Revisiting retinoblastoma protein phosphorylation during the mammalian cell cycle. *CMLS-Cell Mol Life Sci* **58**, 580–595 (2001).
34. Poolman, R. A. & Brooks, G. Expressions and activities of cell cycle regulatory molecules during the transition from myocyte hyperplasia to hypertrophy. *J Mol Cell Cardiol* **30**, 2121–2135 (1998).
35. Martínez-Balbás, M. A., Bauer, U.-M., Nielsen, S. J., Brehm, A. & Kouzarides, T. Regulation of E2F1 activity by acetylation. *EMBO J* **19**, 662-671 (2000).
36. AT1R conformation mediates mechanical stress-induced β-arrestin signaling. *Circ Res* **111**, A330 (2012).
37. Lv, H. *et al.* Transcriptome analysis of Chlamydomonas reinhardtii during the process of lipid accumulation. *Genomics* **101**, 229–237 (2013).
38. Oelkers, P., Cromley, D., Padamsee, M., Billheimer, J. T. & Sturley, S. L. The DGA1 gene determines a second triglyceride synthetic pathway in yeast. *J BiolChem* **277**, 8877–8881 (2002).
39. Davis, M. S., Solbiati, J. & Cronan, J. E. Overproduction of acetyl-CoA carboxylase activity increases the rate of fatty acid biosynthesis in Escherichia coli. *J Biol Chem* **275**, 28593–28598 (2000).
40. Sakthivel, R., Elumalai, S. & Mohommad, M. Microalgae lipid research, past, present: a critical review for biodiesel production, in the future. *J Exp Sci* **2**, 29–49 (2011).
41. Illman, A., Scragg, A. & Shales, S. Increase in Chlorella strains calorific values when grown in low nitrogen medium. *Enztme Microb Tech* **27**, 631–635 (2000).
42. Braun, F.-J., Hegemann, P. Direct measurement of cytosolic calcium and pH in living Chlamydomonas reinhardtii cells. *Eur J Cell Biol* **78**, 199–208 (1999).

Author contributions

All authors contributed to the designing of the experiments and to the writing of the main text. S.M. and G.Y. prepared all figures and contributed to writing the main text related that figures. And J.J. prepared some panels of figures and contributed to writing main text

related it. S.S. discussed the results and wrote the discussion section of the text and H.S. supervised this study. All authors reviewed the manuscript.

Additional information

Supplementary information accompanies this paper at http://www.nature.com/scientificreports

Competing financial interests: The authors declare no competing financial interests.